A Study on the Servo Actuator Tracking Control System

Sung-Gun Han
Department of Railway Vehicle system Engineering
Woosong University, Daejeon, Republic of Korea

Hyoung-Eui Kim
Korea Testing Inc., Daejeon, Republic of Korea

Abstract- Our system consists of pneumatic and hydraulic parts, called hybrid actuator systems. The hydraulic brake system can control a piston's speed. This hydraulic system uses an electronic-hydraulic servo valve to control how hydraulic oil is connected to the actuator, and the FPGA-based PID controller allows approximately 0.3 seconds of running time for system requirements. The test results demonstrated the pressure and speed response of the cylinder through nonlinear feedback control. Target tracking results match the test data well. Adjusting control profits can significantly reduce errors.

Keywords – Actuator, Tracking, Servo valve, Target

I. INTRODUCTION

Pneumatic systems are generally made up of cylinders driven by compressed air and can be operated easily and at a low cost. It is also used as a driving device for various mechanical devices because it can generate sufficient force while driving at high speed [1-3]. Using these characteristics, we intend to use a pneumatic servo actuator for more detailed motor control, such as a servo control air pressure system. The hybrid servo actuator (HSA) system used by the authors is a kind of tracking control system. Difficulty in controlling air pressure due to nonlinearity is related to the compressibility of air in the cylinder and the complex distribution of friction by the cylinder[4-7]. The purpose of this study is to control the measurement curve that tracks the target brake pressure and speed profiles of various waveforms used as the input target profile. Precise control of the actuator can ensure that the target tracking control test results and test data match well. Crash testing can lead to important steps in designing new cars. However, high-cost tests will limit the number of collision tests and sufficient test data. The final purpose of this study is to develop essential tools to reduce car development time and cost. The hybrid actuator used in this study consists of a hydraulic brake device to stop the actuator rod temporarily driven by air pressure. This hydraulic brake system should be able to adjust the pressure quickly and freely according to the waveform moving forward by the actuator rod. In the servo actuator, the speed control of the actuator was adopted as a meter-out control method to adjust the speed at the outlet side of the actuator.

II. SYSTEM CONFIGURATION AND OPERATING PRINCIPLES

2.1 Configuartion and operating principles –

Figure 1 shows a 3D drawing of a servo actuator including a cylinder of a pressure chamber. The volume of the chamber is determined by the actuator passing through the actuator rod. In addition, the device consists of a brake system for controlling braking force during test driving and an actuator rod acting on the brake system. Because a small amount of hydraulic oil is used, servo valves are used and installed directly into the brake system. The brake system for hydraulic control of braking force is connected to the hydraulic power unit (HPU), and the HPU consists of a pump and a hydraulic axial compressor to first generate the required pressure. The HPU is equipped with a speed sensor to measure the load speed. The test equipment consists of a test mechanism that installs a test specimen in three parts, a durability control panel that supplies and controls pneumatic and hydraulic power, and a LabVIEW Software & NI DAQ system that controls, displays, and acquires the test system.

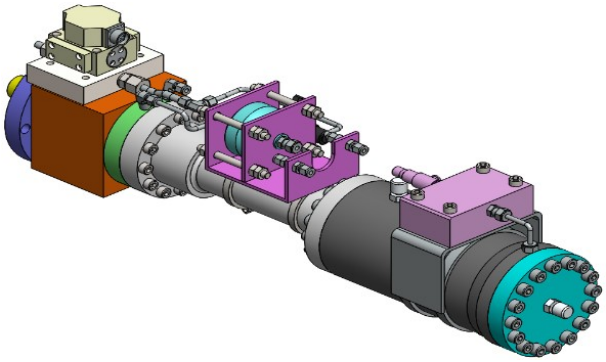

Figure 1. 3D drawing of the servo actuator

The configuration of the test mechanism consists of a high-pressure air compressor that supplies high-pressure air to the servo actuator, a low-pressure air compressor that supplies low-pressure air to the servo actuator, and a high-pressure device that supplies hydraulic power to the brake system for the actuator rod braking and speed control. It also consists of a pressure sensor that measures high pressure and low pressure, a speedometer that measures the actuator load speed of the servo actuator, a proportional pressure control valve that precisely controls hydraulic pressure, a proportional pressure control valve that precisely controls pneumatic pressure and a shock-absorbing pad. A bracket is used to protect equipment in case of rod impact. The FPGA in Figure 2 is a device for controlling the hydraulic servo valve and receiving speed data in a short time, and the DAQ model is responsible for all control devices such as servo valve, pneumatic pressure, hydraulic pressure, etc., excluding speed. For hydraulic servo valves, the FPGA and DAQ modules are separated to perform sensitive millisecond control commands.

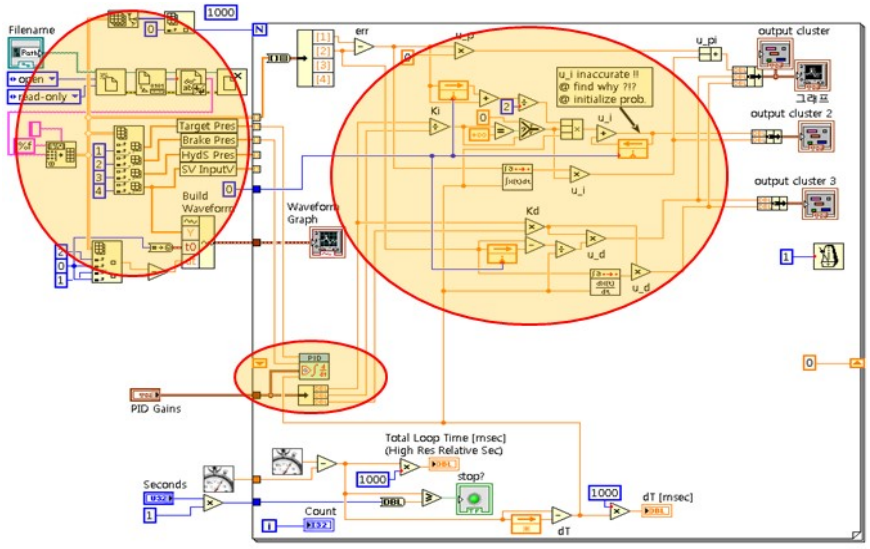

Figure 2. FPGA target configuration

Figure 3 shows a graphical user interface (GUI) developed with LabVIEW. This GUI targets real-time targets for NicRIO-9067 and acquires main control algorithms and data from FPGA targets. The basic firing principle of the actuator rod can be expressed as follows. The low-pressure compressor receives compressed air to return the piston, and the pressure sensor supplies the return pressure to the set pressure. Therefore, the position of the actuator rod is detected by the proximity sensor to prepare for launch. The gate valve opens and the cushion oil is filled through the servo valve. Then, the pressure sensor checks the set pressure. To charge the hydraulic accumulator, the HPU operates with the servo valve in a neutral position and the gate valve open. The hydraulic accumulator is charged and the set pressure is confirmed by the pressure sensor. The brake piston operates as the servo valve position changes. The high-pressure compressor operates to charge the high-pressure air tank. The hydraulic servo valve releases the brake and ignites the actuator rod. The speedometer detects the speed of the actuator rod. The operation

of the servo valve performs an effective operation stroke of the actuator rod and releases backpressure. The brake piston operated and the actuator rod is braked by a change in position of the servo valve.

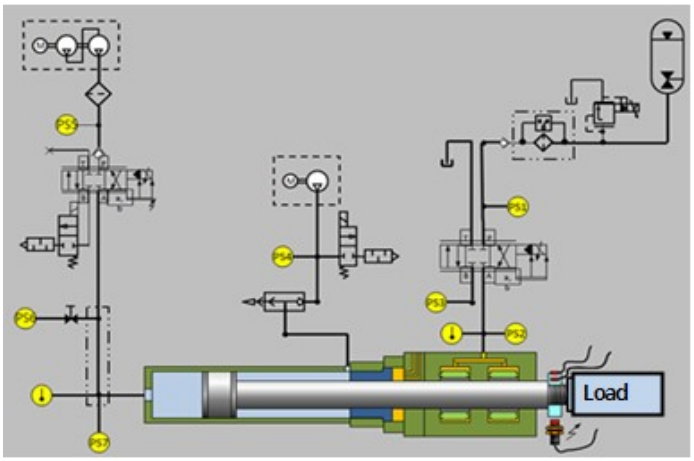

Figure 3. Block diagram of the system developed by LabVIEW

2.2. Sensor noise and noise elimination

Noise is always present in all electronic devices that transmit or receive signals. Our system has many pressure sensors used to show users the operation of the system, basically returning the signal shown in Figure 4.

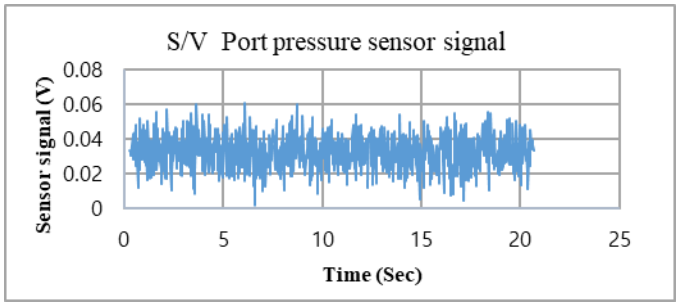

(a)

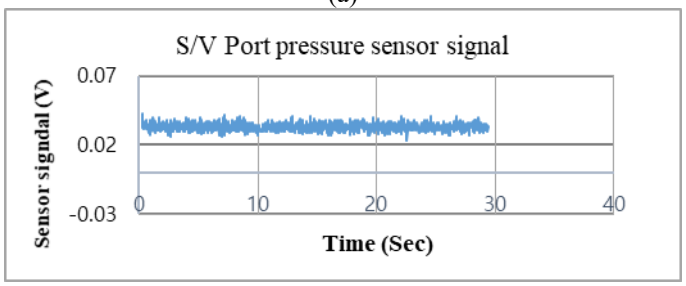

(b)

Figure 4. Noise reduction (a) without low pass filter (b) with a low pass filter

The figure 4 shows raw data and filtered data by a low-pass filter. Using a low filter reduces noise in the filter raw data by about 5 times as shown in Table 1. A low pass filter is used to substantially eliminate or reduce sensor noise in the servo valve (S/V). A low pass filter is a filter that passes a signal of a frequency lower than a specific cutoff frequency and attenuates a signal of a frequency higher than the cutoff frequency. The amount of attenuation for each frequency is related to the filter design.

Table -1 Comparison table for standard deviation and variance with and without filter

	Standard deviation	Variance
Without low pass filter	**σ=0.009714**	**σ^2=9.4x10^{-5}**
With pass filter	**σ=0.002106**	**σ^2=7.3x10^{-6}**

2.3.PIDcontrol tracking algorithm

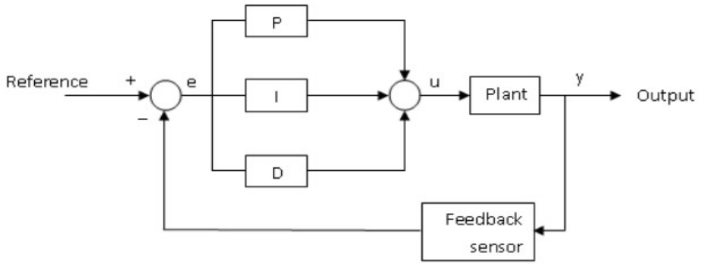

Figure 5. PID algorithm

Figure 5 shows the PID control structure for our hydraulic servo actuator system. Labview shows that this approach based on nonlinear feedback control designs and well-known PID control circuit designs for closed-circuit controllers applies well to bandwidth systems. The target tracking speed RMS error formula is expressed by the following formula, and X means velocity.

$$RMSE = \sqrt{\frac{\sum(X_{target\_i} - X_{tracking\_i})^2}{n}}$$

Figure 6 shows the arrangement of velocity error configurations. LabVIEW is a powerful programming software in the industry for system automation and data acquisition.

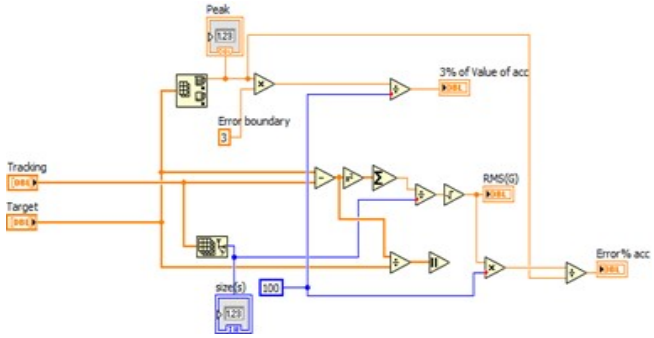

Figure 6. Speed error array

We used NI-Compact with the advantages of LabVIEW FPGA.RIO 9067 real-time target system with FPGA targets. In order to replace a vehicle collision test with a simulator, the simulator must be able to simulate an accurate situation. The way to simulate a collision situation is to generate the same speed in the simulator. Therefore, there is a need for a control algorithm to track the speed profile measured in the collision situation in the actuator of the simulator. User graphics interfaces were developed using the LabVIEW program to execute the developed speed tracking algorithm. The servo actuator system tracking controller includes a model-based tracking control controller that accurately tracks measured speeds at the desired speed using feedforward and feedback controls as external loop controllers around the servo system. The block diagram of the model-based tracking control algorithm is shown in Figure 7.

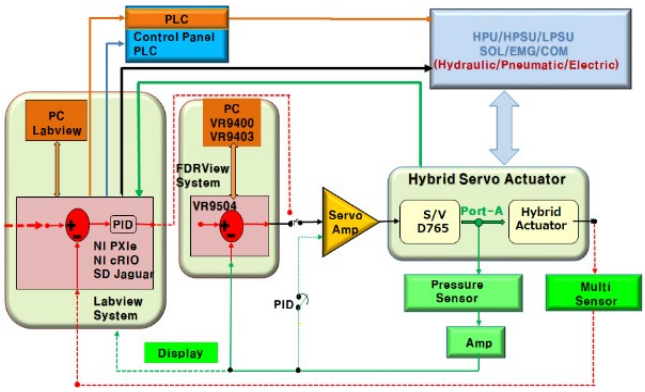

Figure 7. Model based tracking control algorithm

The way to simulate a collision situation is to generate the same speed in the simulator. Therefore, there is a need for a control algorithm to track the speed profile measured in the collision situation in the actuator of the simulator. User graphics interfaces were developed using the LabVIEW program to execute the developed speed tracking algorithm. The servo actuator system tracking controller includes a model-based tracking control controller that accurately tracks measured speeds at the desired speed using feedforward and feedback controls as external loop controllers around the servo system. The block diagram of the model-based tracking control algorithm is shown in Figure 7.

III. Experiment and Result

In order to obtain the results most similar to the actual collision test, accurate modeling of vehicle collision propulsion must take precedence. This technology development study presents a simulator controller algorithm that generates speed signals in reverse in vehicle collision situations. Turn on the HPU and charge the accumulator with working oil. The actuator stores compressed air in the air tank for actuator rod launch. The brake system brakes the rod until the operator fires the actuator rod. When the actuator is activated, the compressed air presses the actuator and the brake system releases the brake until the actuator starts controlling the speed using the brake system.

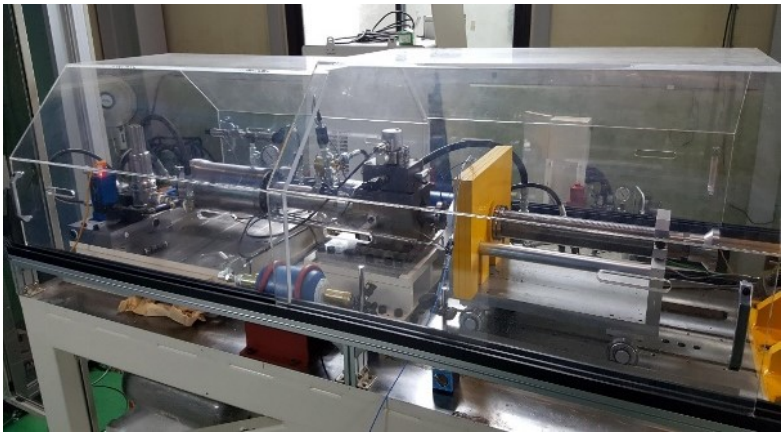

Figure 8. Photograph of servo actuator test equipment

Figure 8 is a picture of the servo actuator test equipment. To control and track speed and pressure profiles using manipulated collision test equipment, connect to LabVIEW using the AMESim program to obtain experimental data. The current system uses open circuits for pressure controllers and closed circuits for speed control loops. In the case of PID control, the loop was executed at a speed of 2.5 mm sec, and the P, I, and D gain values were set to 0.43, 0.001, and 0.000, respectively. The valve and air chamber supply pressures are about 200 bar and 25 bar, respectively. The primary goal of our experiment is to verify the servo valve characteristics and system execution tests. The maximum process time to run a cycle of the loop without a time delay is 78μs. We did several

experiments with servo valves used in hydraulic brake systems. First, the input target profile was selected as a function of sine waves. Figure 9 shows the actual measurement curve that tracks the target brake pressure profile of the sine wave at 20 Hz. The RMS error of the sine wave's target brake pressure was 0.93 bar. This value meets the desired margin of error. Second, the input target profile was selected as a function of a triangular waveform. Figure 10 shows the actual measurement curve tracking the target brake pressure profile of the triangular waveform. The target brake pressure of the triangular wave was 1.15 bar of RMS error. This value also meets the desired error limit. Third, the input target profile was selected as a function of the lamp and step waveform as shown in Figure 11. The RMS error of the target brake pressure of the lamp and stage waveform was 1.43 bar. This value also meets the desired error limit. Finally, the input target profile was selected as a function of the step waveform. The RMS error of the target brake pressure of the step waveform was 3.42 bar. The RMS error value of the step waveform did not meet the desired error limit. Therefore, the servo valve response is suitable for sine, lamp, and triangular waveform, but the step waveform response is poor. PID does not appear to completely overcome the nonlinearity of the brake system in speed tracking. Therefore, the remaining nonlinear conditions of the system must be supplemented.

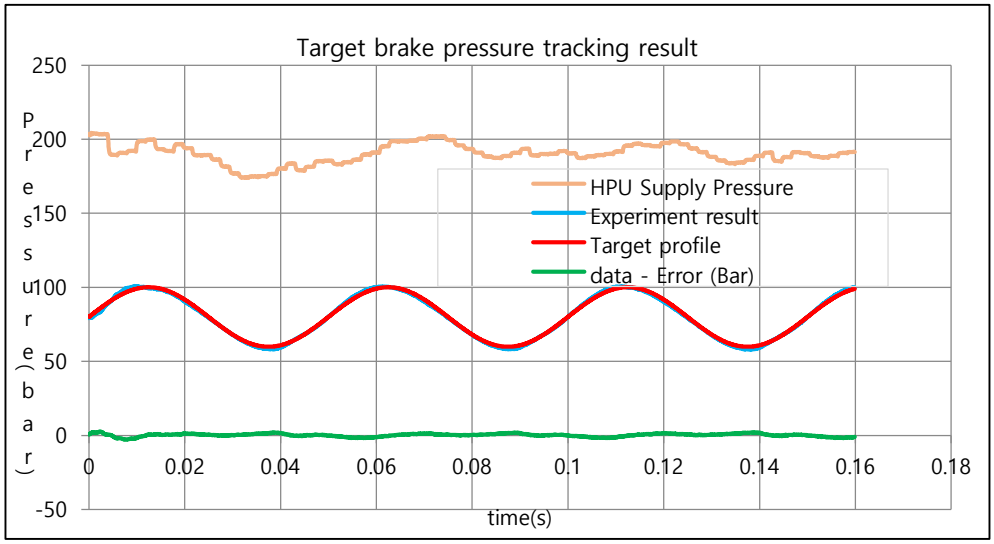

Figure 9. Sinewave signal tracking of target brake pressure

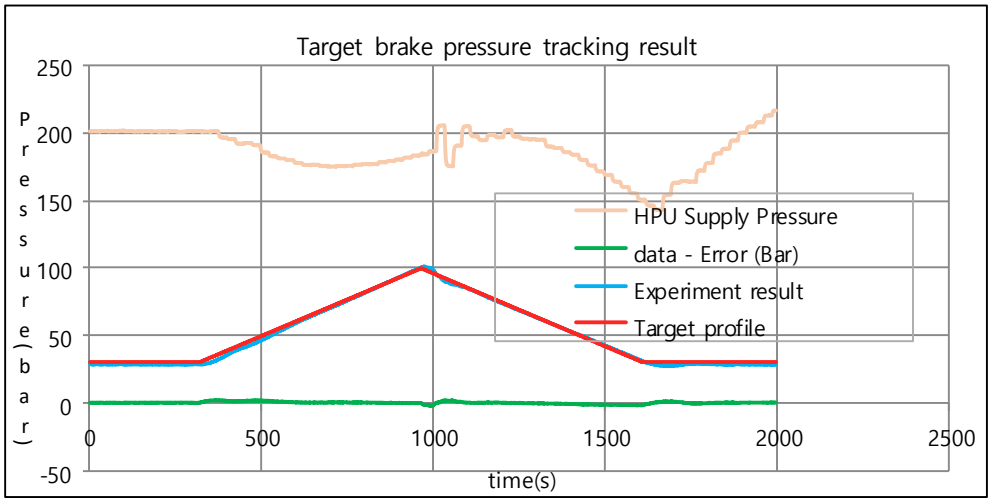

Figure 10. Triangular waveform signal tracking of target brake pressure

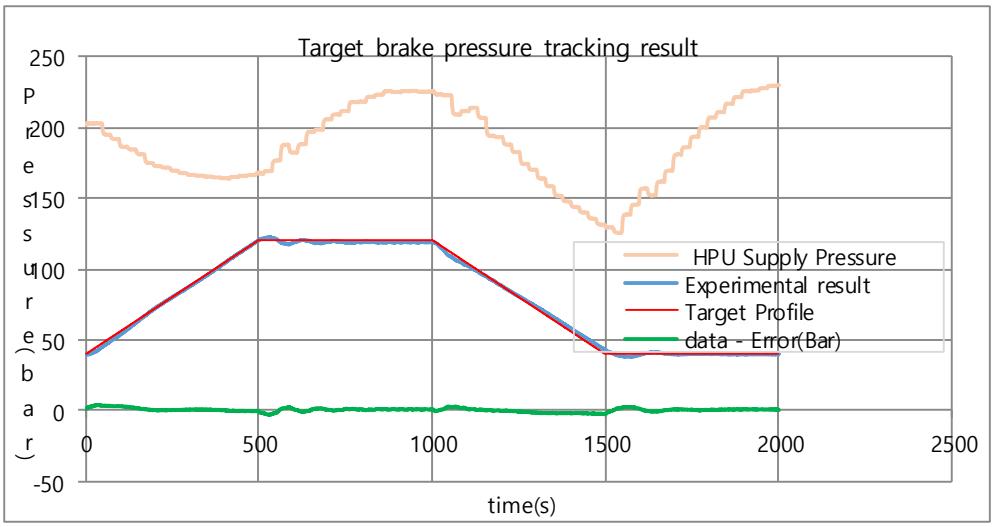

Figure 11. Ramp and step waveform signal tracking of target brake pressure

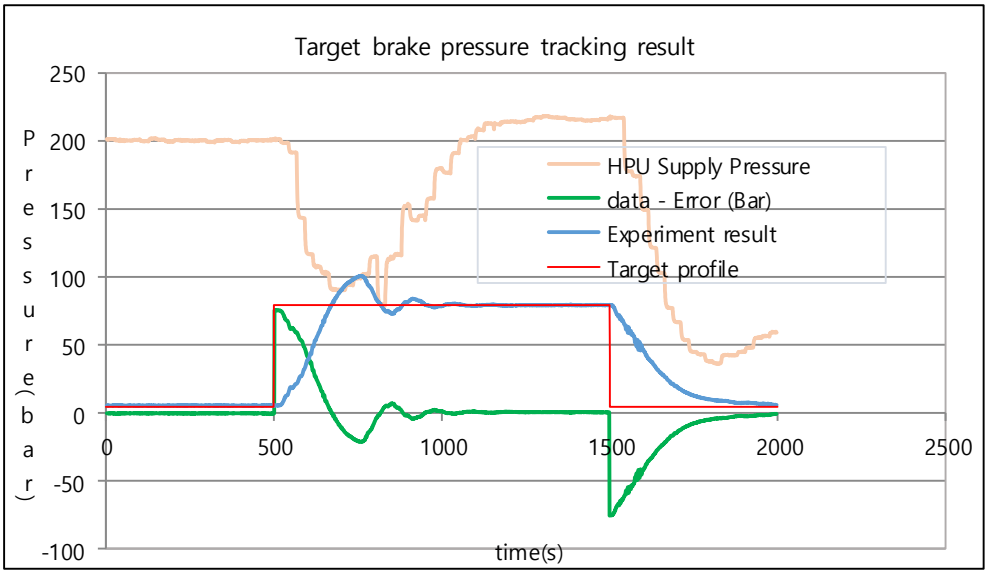

Figure 12. Step waveform signal tracking of target brake pressure

Table -2 Comparison table for errors in various waveform types

Waveform	Target value limit (%)	Test result RMS error (%)
Sine	3	0.93
Triangle	3	1.15
Ramp and step	3	1.3
Step	3	3.42

Table 2 summarizes the comparison of errors in various waveform types. The stage waveform had a large RMS error, as shown in Figure 12, but as shown in Figure 13, the target tracking rate was found to follow the target waveform well. As a result of comparing the graphs of Figure 13(a) and (b), it can be seen that the adjustment of the control gain relatively significantly reduced the error. Therefore, the actual experiment shows that it is necessary to

adjust the control gain as shown in Figure 13. For the optimal performance of the PID, the control variable was set appropriately. There is an unexpected delay in tracking. It may be related to the mechanical portion of the brake system and the reaction of the servo valve. First, it is removed from the closed-circuit loop state and increases at a very small value, which increases until the system response increases this value. The remaining variables are set using the system characteristics that appear during critical vibration.

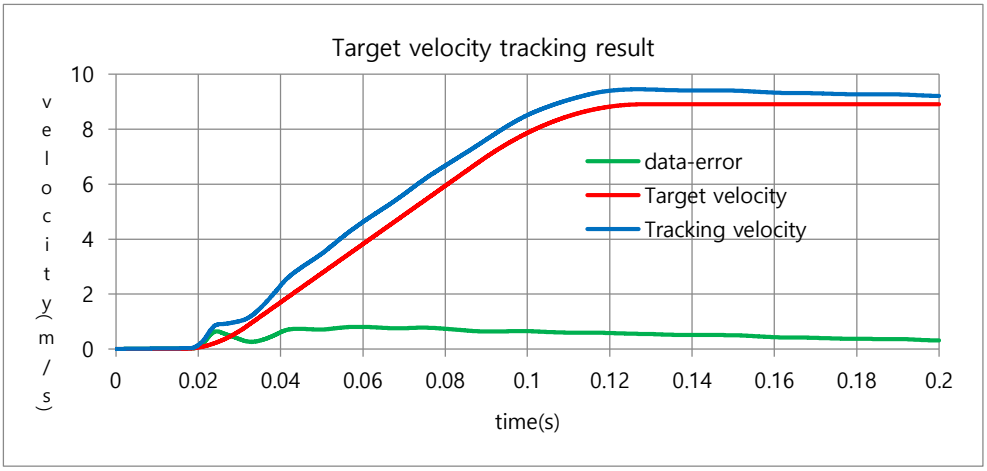

(a) P=0.26, I=0.001, D=0.000

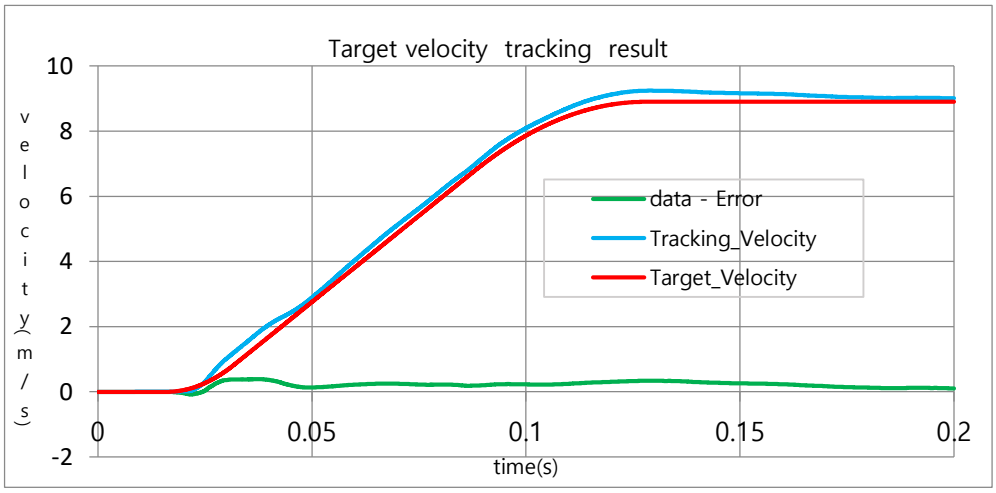

(b) P=0.43, I=0.001, D=0.000

Figure 13. Adjustment of PID control gain

IV.CONCLUSION

After conducting the experiment, we concluded as follows. The design of the FPGA-based PID controller was consistent with the assumptions of system requirements, allowing testing within about 0.3 seconds. As a result of the experiment, in the case of waveforms other than the step waveform, the RMS error between the target pressure profile and the measured pressure meets the target value limit. PID gain adjustment is related to the target tracking pressure, and the supply pressure of the servo valve also affects the PID gain selection. In addition, PID gain adjustment allowed precise control of actuator load speed. Therefore, control errors can be improved through control gain adjustment. Sometimes unexpected time delays exist in tracking. This may be related to the mechanical portion of the braking system and the reaction of the servo valve. As a simulator developed based on an actuator load speed tracking experiment, it can lead to the development of a new vehicle.

REFERENCES

[1] M. Weickgenannt, N.Zimmert, S. Klumpp, O. Sawodny, “Application of SDRE control to servopneumatic drives”, 2010 IEEE International Conference on Control Applications(CCA), Yokohama, Sept.8-10, 2010.

[2] Jay F. Hooper, “Basic Pneumatics: an introduction to industrial Compressed Air Systems and Components”, Carolina Academic Press, 2003.

[3] W. Qiong, Z. Jiao, “Modeling and analysis of pneumatic loading system”, International Conference on Fluid Power and Mechatronics (FPM), Beijing, Aug. 17-20, 2011.

[4] Y. Liu, J. Li, Z. Zhang, X. Hu and W. Zhang, “Experimental comparison of five friction models on the same test-bed of the micro stick-slip motion system”, Mechanical Sciences, vol. 6, No. 1, p. 15-28, 2015.

[5] B. Armstrong-Helouvry, “Control of machines with friction”, Springer Science & Business Media, vol. 128, 2012.

[6] B. Armstrong-Helouvry, P. Dupont, and C. C. De Wit, “A survey of models, analysis tools and compensation methods for the control of machines with friction”, Automatica, vol. 30, No. 7, pp. 1083-1138, 1994.

[7] D. A. Haessig and B. Friedland, “On the modeling and simulation of friction”, Journal of Dynamic Systems, Measurement, and Control, vol. 113, No. 3, pp. 354-362, 1991.